ELSEVIER

Biophysical Chemistry 105 (2003) 339–359

Biophysical Chemistry

www.elsevier.com/locate/bpc

Molecular simulation study of cooperativity in hydrophobic association: clusters of four hydrophobic particles☆

Cezary Czaplewski[a,b], Sylwia Rodziewicz-Motowidło[b], Magdalena Dąbal[b], Adam Liwo[a,b], Daniel R. Ripoll[c], Harold A. Scheraga[a,*]

[a]*Baker Laboratory of Chemistry and Chemical Biology, Cornell University, Ithaca, NY 14853-1301, USA*
[b]*Faculty of Chemistry, University of Gdańsk, ul. Sobieskiego 18, Gdańsk 80-952, Poland*
[c]*Cornell Theory Center, Ithaca, NY 14853-3801, USA*

Received 9 September 2002; accepted 13 November 2002

Abstract

The multibody contribution to the potential of mean force (PMF) of hydrophobic association of four methane molecules in water was investigated by means of umbrella-sampling molecular dynamics. Two systems were considered: (i) a trigonal pyramid with three methane molecules at contact distance forming a fixed base, the fourth molecule being placed on the top with variable distance from the base; and (ii) a regular uniformly expanding tetrahedron. Methane–methane distances as far as 12.5 Å, i.e. beyond the second solvent-separated minimum of the PMF, were considered to address the baseline problem. In contrast to the small effect in the three-body case studied previously (Protein Sci 9 (2000) 1235), the multibody contribution was found to amount to approximately 0.2 kcal/mol per methane–methane pair, or approximately 25% of the depth of the contact minimum in the PMF. The main effect of the multibody contribution to the PMF is a reduction of the height of the barrier between the contact and solvent separated minima and a narrowing of the region of its maximum, while the region of the contact minimum is affected only weakly. The reduction of the barrier is due to four-body contributions. The cooperative contributions to the PMF agree very well with those computed from the molecular surface of the systems under consideration, which further supports earlier observations that the molecular surface can be used with good accuracy to describe the energetics of hydrophobic association.

Keywords: Hydrophobic association; Potential of mean force; Cooperativity; Molecular surface

1. Introduction

Kauzmann's seminal review of solvent effects on the denaturation of proteins [1], following his earlier statement [2], which did not reach as wide an audience, increased awareness of the concept of hydrophobic interactions. Kauzmann used the term 'hydrophobic bonding' to describe the tendency of the non-polar groups of proteins to adhere to one another in aqueous environment. The hydrophobic effect may be defined as the behavior of

☆ This article is dedicated to Walter Kauzmann for his seminal contributions to bio-physical chemistry.

*Corresponding author. Tel.: +1-607-255-4034; fax: +1-607-254-4700.

E-mail address: has5@cornell.edu (H.A. Scheraga).

0301-4622/03/$ - see front matter © 2003 Elsevier Science B.V. All rights reserved.
doi:10.1016/S0301-4622(03)00085-1

non-polar solutes in aqueous solution, and the term usually refers to both hydrophobic hydration and hydrophobic interactions [3–6]. Hydrophobic hydration concerns the interactions of one non-polar molecule with its aqueous environment, i.e. modification of the structure and dynamics of water due to the presence of a solute molecule, and the resulting thermodynamic changes. Hydrophobic interactions, the term more commonly used today, rather than hydrophobic bonding coined by Kauzmann, refer to the attractive potential of mean force (PMF) that acts between two or more non-polar molecules in aqueous environment.

Kauzmann [1,2] has proposed that hydrophobic interactions are one of the more important factors stabilizing native protein structure. Since then, it has long been accepted that the hydrophobic effect is of fundamental importance in the molecular mechanism of stability of various self-assembly aggregates and biological structures in aqueous environment. It plays an important role in many biophysical phenomena, such as protein folding, the formation of micelles, biological membranes and macromolecular complexes, molecular recognition, coagulation and surfactant aggregation [6–11]. Hydrophobic interactions are the most familiar subset of more general solvent-induced interactions, i.e. indirect interactions among solutes, caused by the presence and the particular nature of the solvent. Solvent-induced interactions between hydrophilic groups have not received as much attention as hydrophobic interactions. Ben-Naim claimed that the importance of hydrophobic interactions is over-exaggerated based upon over-estimates of their magnitude and that hydrophilic effects (both solvation and correlation) might be much more important in biochemical processes [12,13]. Yet a closer examination [14] of water-bridge-induced hydrophilic interactions, which he had proposed, did not provide sufficient evidence for such a conclusion.

Influenced by discussions with Kauzmann and Linderstrøm-Lang at the Carlsberg Laboratory in 1957, and by papers of Frank and Evans [15] and Frank and Wen [16], Némethy and Scheraga began a series of statistical machanical investigations of the thermodynamics properties of liquid water [3,17] and aqueous solutions of hydrocarbons [18], as a basis for computing the free energy, enthalpy, entropy and heat capacity for pairwise- and multi-body hydrophobic bonds (interactions) involving non-polar amino acid side chains of varying size [19]. This statistical mechanical treatment was based on a model, the most important feature of which was the flickering cluster (partial cage or clathrate) picture proposed by Frank and Wen [16]. However, subsequent Monte Carlo [4,5] and molecular dynamics [20,21] simulations of aqueous solutions of inert molecules verified the validity of this model. Scheraga has recently summarized this work [11], including experimental results that verified the thermodynamic parameters that had been calculated by Némethy and Scheraga [19].

Despite tremendous effort by both experimentalists and theoreticians, there is still much to be learned about the hydrophobic phenomenon on a molecular level. Frank and Evans [15] and Némethy and Scheraga [3] demonstrated that hydration of a small hydrophobic solute involves a large heat capacity because the mechanism of hydration of a small non-polar solute changes with increasing temperature from entropic (ordering of neighboring waters) to enthalpic (breaking of hydrogen bonds among the neighboring waters) [11,18,19]. By contrast, water molecules hydrate a large hydrophobic solute (the extreme example being a planar hydrophobic surface) with rupture of the hydrogen bonds being independent of temperature [22–24].

Némethy and Scheraga [19] noticed that hydrophobic interactions between more than two solute particles are not pairwise. Later, Lum et al. [25] also showed that, when the local concentration of hydrophobic units is large enough or each hydrophobic particle has a sufficiently large surface, these can induce ‘drying’, which leads to strong attractions between large non-polar objects, as observed in surface force measurements. The structure of water near small non-polar species provides little information about the phenomenon that dominates for larger hydrophobic assemblies. Drying is a collective phenomenon, and a pair potential of mean force between small non-polar units cannot characterize such an effect.

Quite often a distinction is made between pairwise and bulk hydrophobic interactions, i.e. according to the scale of the phenomenon [6,19,25,26]. A pairwise PMF is adopted for the interactions among small non-polar groups while bulk hydrophobic interactions describe exposure of hydrophobic residues from its pure phase to water [19]. These differences are not always recognized as qualitative [27] and should rather be regarded as extreme cases of a single phenomenon. The change of the character of hydrophobic association with increasing size of the cluster must, therefore, be a result of multibody contributions to hydrophobic forces [19]. Most of the studies of hydrophobic interactions at the molecular level characterize only the pairwise PMF for two nonpolar particles in aqueous solution [4,21,28–30], and its dependence on the environmental variables, such as temperature [19,31,32], pressure [33,34] or ionic strength of the solution [35]. For a better understanding of complex hydrophobic phenomena, it is necessary to look beyond single-solute hydration and pairwise PMF.

The first simulations of the PMF of three hydrophobic particles in water using the free energy perturbation (FEP) method and the TIP4P water model have shown that the three-body term is nonzero [36], but Rank and Baker were not able to determine its value unequivocally. The errors associated with baseline estimation, i.e. the zeroing of the absolute free energies at long distances, were reported to be of the same order of magnitude (0.2–0.3 kcal/mol) as the three-body term itself. Our molecular-dynamics study of hydrophobic association using umbrella sampling and the weighted histogram analysis method (WHAM) with the methane molecule as a model of a hydrophobic solute and two water models (TIP3P and TIP4P), showed that hydrophobic interactions cannot be described by a pairwise potential, and that a three-body contribution increases the strength of hydrophobic association by approximately 10% [37].

Shimizu and Chan presented the results of a particle-insertion simulation of the hydrophobic effect using the TIP4P water model, which suggested that there is significant anti-cooperativity in hydrophobic interactions [38], (i.e. that the deviation of the free energy of hydrophobic interactions among three particles from pairwise additivity is positive, thereby weakening the hydrophobic interactions). This result contradicted that of our molecular simulation study of the hydrophobic effect, which revealed strengthening of hydrophobic interactions [37]. The results depend critically on the estimation of the free energy of the zero reference state. The baseline corresponds to the value of the free energy of hydration of a hydrophobic particle, which Shimizu and Chan estimated by the particle-insertion method, while in our study, we estimated the baseline of the cooperative term in the PMF by assuming that the cooperative term vanishes with distance faster than the PMF itself. Shimizu and Chan consider their method of baseline estimation superior to ours.

We have criticized [39] Shimizu and Chan for not presenting any estimate of the errors of the pairwise PMF used for calculating the three-body term and for neglecting the minimum-image convention, which restricts the maximum separation of solute molecules in the simulation box to half of the box dimension when analyzing the results of simulations. Additionally, we studied a second model system with methane molecules on the vertices of an equilateral triangle (the m+m+m system, Fig. 1, which is restrained, but not constrained to equilateral), and found that the three-body term strengthens the hydrophobic interactions [37]. Recently [40], we carried out simulations of a larger hydrophobic solute in water, constituting the system analogous to m+m+m (Fig. 1). As in our study of the methane trimer [37], we found that the three-body term increases the strength of hydrophobic interactions. The simulations were carried out in a 28 Å periodic box with solute–solute distances up to 14 Å, where all PMF curves become flat within the error inherent in simulations, which provided for a reliable estimate of the baseline.

In reply to our comment [39], Shimizu and Chan [41] presented an estimation of the numerical uncertainties of their two-methane PMF, which was missing in their previous paper [38], and agreed that the accuracy of their two-methane PMF had to be improved in order to provide better accuracy of the three-body term. However, they

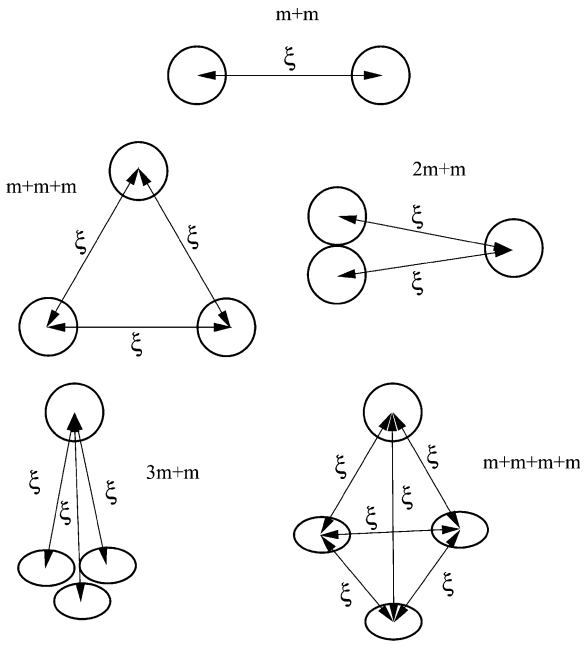

Fig. 1. Scheme of the methane clusters studied; ξ is the reaction coordinate. See text for explanation.

concluded that, even given the limited simulation data available to date, there is stronger support in favor of anti-cooperativity than cooperativity for a significant fraction of the three-methane configurations that they had investigated. In their most recent paper [42], Shimizu and Chan presented a full free energy landscape for a fixed methane dimer and an approaching methane molecule. They revised their two-methane PMF to a higher accuracy than the ones used in their previous study [38] and added one additional PMF for another three-methane system with a methane molecule approaching the methane dimer along the line connecting two methane molecules in the dimer [42]. Apart from this, they used the same data for the three-methane PMFs as in their previous paper [38] and have not addressed the issue of edge effect close to half of the box distance but cut all curves at 11 Å (previously, the same data were presented up to the 13 Å distance [38]). Their two-methane PMF curve is now similar to ours [37,39,40] and their three-body PMF curve is shifted up by approximately 0.1 kcal/mol. Shimizu and Chan [41,42] tried to explain this by long-range effects in hydrophobic association. According to them, these long-range effects can be captured by the test-particle-insertion method, which provides an absolute association energy (not directly but by taking into account the free energy of hydration of a single hydrophobic particle as a reference). They admitted [42] that a larger simulation box should be used to prove that hydrophobic association is mostly anti-cooperative. Nevertheless, the spatial range of hydrophobic interactions is finite and the PMF must tend to zero with increasing solute–solute distance. As shown in Section 3 presented here, distances larger than 10.5 Å, where it is possible to observe the second solvent-separated minimum, are large enough to show that the PMF curves become flat.

The cooperativity effects in solvent-induced forces (SIF, the negative of the PMF gradient) have been the focus of investigations of Palma and coworkers [43,44]. They found an inherently strong non-additivity of SIF in water. The departures of SIF from additivity are comparable to the SIFs themselves, and a correct account for this requires introducing multibody contributions to the PMF. Two more studies of multibody effects in hydrophobic association were carried out by Levitt and co-workers [45,46], but their investigation focused on the total free energy of association and not on the distance dependence of the PMF.

Most models used thus far in theoretical studies of protein structure oversimplify the true nature of the hydrophobic interactions conceived of long ago by Kauzmann and ignore their multibody character. The importance of accounting for non-additive effects in protein folding should be emphasized. Purely pairwise contact potentials are insufficient for ab initio protein-structure prediction [47]. For large enough databases, the pairwise contact approximation to the free energy cannot stabilize all the native folds even against the decoys obtained by gapless threading [48,49]. Skolnick, Kolinski and co-workers [50–52] have studied the importance of non-pairwise multibody interactions and derived the multibody terms on a heuristic basis. Recently, we developed a general method to derive multibody site–site potentials [53], and derived analytical expressions for the

multibody terms pertaining to the correlation between local and electrostatic interactions within the polypeptide backbone. Together with hydrogen-bonding cooperative terms implemented earlier in our united-residue (UNRES) force field [54], the new multibody terms enabled us to carry out de novo predictions of protein structure with both α-helical and β-sheet segments [55]. Without the cooperative terms, the UNRES force field was capable of recognizing only the native structure among the decoys derived by threading from the Protein Data Bank [56], but was not capable of producing correct structures in de novo simulations.

In this study, we concentrate on the thermodynamics of multibody hydrophobic interactions. To investigate the PMF of many body interactions, we simulated the formation of a trimer and a tetramer of methane molecules in explicit water. We carried out simulations in a larger periodic box than before in order to address the baseline estimation problem.

2. Methods

2.1. Definition of cooperativity in hydrophobic association

In a general case of n solute particles in a solvent, the potential of mean force (PMF), $W(\xi)$, of their interaction depends on the vector of variables, ξ, and is defined by the following equation:

$$W(\boldsymbol{\xi}) = -RT\ \ln P(\boldsymbol{\xi},p,T,V) \tag{1}$$

where $P(\boldsymbol{\xi})$ is the conditional probability density of the variables of interest at a given value of $\boldsymbol{\xi}$; p, T and V are the pressure, temperature and volume of the system, and

$$P(\boldsymbol{\xi},p,T,V) = \frac{\int_{V_{\boldsymbol{\xi}}} \exp(-H(\mathbf{x})\mathrm{d}V)}{\int_{V} \exp(-H(\mathbf{x})\mathrm{d}V)} \tag{2}$$

where H is the Hamiltonian of the system (solute plus solvent), V is the volume of the whole configurational space of the system, and $V_{\boldsymbol{\xi}}$ is the volume of the fraction of the configurational space restricted to $\boldsymbol{\xi}$. If P is evaluated at constant pressure and temperature, the potential of mean force, W, corresponds to the restricted Gibbs free energy of the system, while for constant volume and temperature it corresponds to the restricted Helmholtz free energy. Throughout this paper, we identify the PMF with the restricted Helmholtz free energy.

The potential of mean force W of an n-particle interaction can be decomposed into single-body, pairwise and multibody terms:

$$\begin{aligned} W(1,2,\ldots,n) &= F(1,2,\ldots,n) - \sum_{i}^{n} F^{(1)}(i) \\ &= \sum_{i<j}^{n} \delta F^{(2)}(i,j) + \sum_{i<j<k}^{n} \delta F^{(3)}(i,j,k) \\ &\quad + \cdots + \sum_{i<j<\ldots}^{n} \delta F^{(l)}(i,j,\ldots) \\ &\quad + \delta F^{(n)}(i,j,\ldots,n) \end{aligned} \tag{3}$$

where $F(1,2,...,n)$ is the shorthand for $F(\xi_1, \xi_2,\ldots,\xi_{3n-6})$, ξ_i being the ith reaction coordinate. $F^{(1)}(i)$ corresponds to hydrophobic hydration (serving to define the reference state), $\delta F^{(2)}(i,j)$ is the two-body term of hydrophobic association and $\delta F^{(l)}(i,j,\ldots)$ corresponds to subsequent higher-order terms. In this work, we investigate the two lowest-order cooperative terms, $\delta F^{(3)}$ and $\delta F^{(4)}$.

The three-body term $\delta F^{(3)}$ can be derived recursively from Eq. (3). Given the unnormalized total PMF, $F(r_{12}, r_{13}, r_{23})$, for the cluster of three solute molecules in water (r_{ij} being the site–site distances identified with the respective reaction coordinate), the three-body cooperativity term, $\delta F^{(3)}(r_{12}, r_{13}, r_{23})$, can be expressed as:

$$\begin{aligned} \delta F^{(3)}(r_{12}, r_{13}, r_{23}) &= F(r_{12}, r_{13}, r_{23}) - \delta F^{(2)}(r_{12}) \\ &\quad - \delta F^{(2)}(r_{13}) - \delta F^{(2)}(r_{23}) \\ &\quad - 3F^{(1)} \\ &= F(r_{12}, r_{13}, r_{23}) - 3F^{(1)} \\ &\quad - [F(r_{12}) - 2F^{(1)}] \\ &\quad - [F(r_{13}) - 2F^{(1)}] \end{aligned}$$

$$
\begin{aligned}
&-[F(r_{23})-2F^{(1)}]\\
&=W^{(3)}(r_{12},\, r_{13},\, r_{23})\\
&\quad-[W^{(2)}(r_{12})\\
&\quad+W^{(2)}(r_{13})\\
&\quad+W^{(2)}(r_{23})] \qquad (4)
\end{aligned}
$$

where $F(r_{ij})$ is the unnormalized total PMF for an isolated solute pair in water, $F^{(1)}$ is the hydrophobic hydration free energy of a single solute molecule, which is an unknown constant. Computing the differences $F(r_{12},\, r_{13},\, r_{23})-3F^{(1)}$ and $F(r_{ij})-2F^{(1)}$ is equivalent to shifting the respective total PMFs to zero values at infinite (practically sufficiently large) distances between the solute molecules and provides the normalized PMF, $W^{(3)}(r_{12},\, r_{13},\, r_{23})$ and $W^{(2)}(r_{ij})$, respectively. Thus, $\delta F^{(3)}(r_{12},\, r_{13},\, r_{23})$ can be determined from the difference between the three-body and the sum of two-body normalized PMFs.

Similarly, the four-body term $\delta F^{(4)}(r_{12},\, r_{13},\, r_{23},\, r_{14},\, r_{24},\, r_{34})$ can be expressed as:

$$
\begin{aligned}
&\delta F^{(4)}(r_{12},\, r_{13},\, r_{23},\, r_{13}\, r_{24}\, r_{34})\\
&\quad=W^{(4)}(r_{12},\, r_{13},\, r_{23},\, r_{14}\, r_{24}\, r_{34})\\
&\qquad-[W^{(3)}(r_{12},\, r_{13},\, r_{23})\\
&\qquad+W^{(3)}(r_{12},\, r_{14},\, r_{24})\\
&\qquad+W^{(3)}(r_{13},\, r_{14},\, r_{34})\\
&\qquad+W^{(3)}(r_{23},\, r_{24},\, r_{34})+W^{(2)}(r_{12})\\
&\qquad+W^{(2)}(r_{13})+W^{(2)}(r_{14})+W^{(2)}(r_{23})\\
&\qquad+W^{(2)}(r_{24})+W^{(2)}(r_{34})] \qquad (5)
\end{aligned}
$$

The determination of the PMF of two solute molecules in water is a one-dimensional problem, that of the PMF of three solute molecules is a three-dimensional one, and four solute molecules require six dimensions. In the case of three and four molecules, it is reasonable to study the PMF in a selected one-dimensional subspace. In this article, we considered the same two geometries for the three methane molecules as in our previous work [37]: (a) an equilateral triangle (m+m+m), with the dimension of the triangle being the reaction coordinate ξ; and (b) the three molecules on the vertices of an isosceles triangle (2m+m), with the distance between molecules 1 and 2 restrained to 3.9 Å (the contact-minimum distance between two methane molecules in water) and the distance of the third methane molecule from the first Fig. 1 and the second one, respectively, being the reaction coordinate (Fig. 1). Two cluster geometries were considered for four methane molecules: (c) a trigonal pyramid with an equilateral triangle as a base (the distance between the methane molecules of the base being restrained to 3.9 Å) with the distances between the top and each of the base methane molecules being the reaction coordinate; and (d) a regular tetrahedron with the length of its edges being the reaction coordinate, ξ (Fig. 1). The m+m+m and m+m+m+m systems correspond to uniform expansion or contraction of a hydrophobic cluster while the 2m+m and 3m+m systems correspond to the approach of an additional non-polar molecule to an already formed hydrophobic dimer or trimer, respectively.

2.2. Calculation of the potential of mean force (PMF)

To evaluate the PMF, we used umbrella sampling molecular dynamics (MD) [57,58] with the weighted histogram analysis method (WHAM) [59,60]. In the umbrella-sampling method, a series of restraints (usually harmonic) are imposed on the reaction coordinate to assure that all regions are sampled sufficiently. Each restraint defines a sampling window.

The molecular dynamics umbrella-sampling simulations were carried out using 19 windows with a harmonic restraining potential:

$$V(\xi)=k(\xi-d_o)^2 \qquad (6)$$

with the force constant $k=2$ kcal mol^{-1} Å^{-2} and the 'equilibrium' distance for a given window, d_o, equal to 3.5, 4.0,…, 12.5 Å for windows 1–19. The reaction coordinate ξ was chosen as the solute–solute distance. In the case of the m+m dimer, the m+m+m trimer and the m+m+m+m tetramer, each infra-molecule distance was restrained by Eq. (6) with the same force constant and the same values of d_o as above. In the case of the 2m+m system, umbrella-sampling simulations were carried out by imposing 2 kcal mol^{-1} Å^{-2}

Table 1
Force field parameters for the TIP3P water model [61] and the methane model [62] used in this study[a,b]

Atom type	σ [A]	ε [kcal/mol]	q [eu]
methane			
C4	3.730	0.294	0.0
TIP3P			
HW	0.0	0.0	+0.417
OW	3.1507	0.1521	−0.834

[a] C4 represents the methane molecule, HW and OW represent hydrogen and oxygen atoms of the water molecule, respectively.
[b] The form of the pair potential is $U(r)=4\varepsilon((\sigma/r)^{12}-(\sigma/r)^{6})+q_iq_j(4\pi r)^{-1}$.

restraints on the m_1-m_3 and m_2-m_3 distances with d_o values varying as described above, and a 100 kcal mol^{-1} $Å^{-2}$ restraint on the m_1-m_2 distance with d_o fixed at 3.9 Å (the methane–methane contact-minimum distance in water). Similarly, in the case of the 3m+m systems, 2 kcal mol^{-1} $Å^{-2}$ restraints were imposed on the m_1-m_4, m_2-m_4 and m_3-m_4 distances with d_o values varying as described above and 100 kcal mol^{-1} $Å^{-2}$ restraints on the sides of the base equilateral triangle with d_o fixed at 3.9 Å. Additionally, the internal angles of the equilateral-triangle geometry were restrained to 60° with a harmonic force constant of 100 kcal mol^{-1} rad^{-2} in all systems, i.e. the m+m+m trimer system, four sides of the m+m+m+m tetrahedron and the base of the 3m+m pyramid.

Simulations with methane molecules were carried out by using a cubic periodic box with a 27.6 Å side, and a 9.0 Å cut-off for both the nonbonded and electrostatic interactions. The number of water molecules in the box varied from 694 for m+m to 692 for the m+m+m+m system. The TIP3P model was used for the water molecules, with parameters (Table 1) taken from Jorgensen et al. [61]. Each methane molecule was modeled by a single interaction site, with van der Waals (VDW) parameters [62] listed in Table 1. The VDW parameters of the oxygen–solute interaction were calculated by using the standard Lorentz–Berthelot mixing rules [63], given by:

$$\sigma_{ij}=(\sigma_{ii}+\sigma_{jj})/2 \quad (7)$$

$$\varepsilon_{ij}=\sqrt{(\varepsilon_{ii}\varepsilon_{jj})} \quad (8)$$

where i,j are two different type of atoms, σ and ε correspond to VDW parameters associated with the contact distance and the depth of the well, respectively. The simulations were carried out in the NVT ensemble with temperature at 298 K. The time step in the MD simulations was 2 fs, and a SHAKE algorithm was applied to keep the water molecules rigid [64]. For each umbrella-sampling window, 100 ps equilibration followed by 2000 ps data collection simulations were carried out. The Cartesian coordinates of the solute molecules were stored at every time step of the MD simulation. The simulations were carried out by using the MD module of the AMBER [65] program.

To calculate the PMF from umbrella-sampling simulation data, the data from all simulation windows must be combined, and the contribution due to the restraining potential must be eliminated. We used the weighted histogram analysis method (WHAM) [59,60] as the most advanced approach to this problem. Umbrella-sampling combined with WHAM gives faster convergence and more stable results than other methods [37]. In WHAM, the unbiased probability density corresponding to a given value of the reaction coordinate $\boldsymbol{\xi}$ is computed as a weighted average over all windows. The formulas for the weights [59,60] were derived based on the requirement that the sum of the squares of the errors over all $\boldsymbol{\xi}$ in the calculated distribution be minimized. For a more detailed description of the method, the reader is referred to our previous paper [37] and the original papers by Kumar et al. [59,60].

The bin dimension applied in the WHAM calculations of the PMF was equal to 0.1 Å for the dimer systems (a one-dimensional bin) and trimer systems (three-dimensional bins), while it had to be increased to 0.2 Å for the tetramer systems (six-dimensional bins). For the 2m+m and 3m+m systems, the bins corresponding to the distances within the base of the isosceles triangle or of the trigonal pyramid (3.9 Å), respectively, were placed in the centers of the multidimensional bins corresponding to these variables. This assured that use

was made of all data points close to the subspace of variables considered in the calculation. All points collected from the MD simulations, including those not satisfying the target geometry (the equilateral triangle, the isosceles triangle, the trigonal pyramid and the regular tetrahedron, respectively), were taken to calculate histograms using WHAM. Only the histogram values of the bins whose center positions satisfied the condition required for the target geometry of the systems described above were used for the calculation and visualization of the PMF. Based on Eqs. (1) and (2), the PMF is evaluated from the unbiased histogram obtained from the WHAM method by using Eq. (9).

$$W(\boldsymbol{\xi}) = -RT\ln\frac{N(\boldsymbol{\xi})}{\Delta V(\boldsymbol{\xi})} \tag{9}$$

where $N(\boldsymbol{\xi})$ is the value of the histogram at $\boldsymbol{\xi}$ and $\Delta V(\boldsymbol{\xi})$ is the volume element corresponding to $\boldsymbol{\xi}$. For the two-, three- and four-methane clusters $\Delta V(\boldsymbol{\xi})$ are expressed by Eqs. (10)–(13), respectively.

$$\Delta V_2 = 4\pi d_{12}^2 \Delta d_{12} \tag{10}$$

$$\Delta V_3 = 8\pi^2 d_{12} d_{13} d_{23} \Delta d_{12} \Delta d_{13} \Delta d_{23} \tag{11}$$

$$\Delta V_4 = 16\pi^2 d_{12} d_{13} d_{14} d_{23} d_{24} d_{34} \times \tag{12}$$

$$\begin{aligned}&(d_{13}^2 d_{12}^2 d_{24}^2 + d_{13}^2 d_{23}^2 d_{24}^2 + d_{14}^2 d_{12}^2 d_{23}^2 + d_{14}^2 d_{13}^2 d_{24}^2 \\ &+ d_{13}^2 d_{12}^2 d_{34}^2 + d_{14}^2 d_{12}^2 d_{34}^2 + d_{34}^2 d_{12}^2 d_{24}^2 + d_{34}^2 d_{13}^2 d_{24}^2 \\ &+ d_{34}^2 d_{23}^2 d_{14}^2 + d_{14}^2 d_{13}^2 d_{23}^2 + d_{14}^2 d_{23}^2 d_{24}^2 + d_{34}^2 d_{12}^2 d_{23}^2 \\ &- d_{13}^2 d_{24}^2 - d_{14}^2 d_{23}^2 - d_{34}^2 d_{23}^2 d_{24}^2 - d_{13}^2 d_{24}^2 \\ &- d_{34}^2 d_{13}^2 d_{14}^2 - d_{14}^2 d_{23}^2 - d_{34}^4 d_{12}^2 - d_{34}^2 d_{12}^4 \\ &- d_{14}^2 d_{12}^2 d_{24}^2 \\ &- d_{13}^2 d_{12}^2 d_{23}^2)^{-1/2} \Delta d_{12} \Delta d_{13} \Delta d_{14} \Delta d_{23} \Delta d_{24} \Delta d_{34}\end{aligned} \tag{13}$$

where d_{ij} denotes the distance between solute particles i and j. For the specific cases of the 2m+m, m+m+m, 3m+m and m+m+m+m systems the volume elements are defined by Eqs. (14)–(17), respectively.

$$\Delta V_{2\mathrm{m}+\mathrm{m}} = 8\pi^2 d\xi^2 \Delta\xi^3 \tag{14}$$

$$\Delta V_{\mathrm{m}+\mathrm{m}+\mathrm{m}} = 8\pi^2 \xi^3 \Delta\xi^3 \tag{15}$$

$$\Delta V_{3\mathrm{m}+\mathrm{m}} = 16\pi^2 d(3\xi^2 - d^2)^{-1/2} \xi^3 \Delta\xi^6 \tag{16}$$

$$\Delta V_{\mathrm{m}+\mathrm{m}+\mathrm{m}+\mathrm{m}} = 16\pi^2 2^{-1/2} \xi^3 \Delta\xi^6 \tag{17}$$

where d is the length of the base of the equilateral triangle for the 2m+m system and the edge of the base of the trigonal pyramid for the 3m+m system and $\Delta\xi$ is the bin size assumed equal in all dimensions. It should be noted that Eqs. (14)–(17) imply that the accuracy of the histograms of the 2m+m and 3m+m systems deteriorates with increasing ξ compared to that of the m+m+m and m+m+m+m systems, respectively. This occurs because the volume elements for 2m+m and 3m+m increase more slowly with ξ compared to that of the m+m+m and m+m+m+m systems, respectively, which results in fewer data. For example, with $d = 3.9$ Å the ratios $\Delta V_{\mathrm{m}+\mathrm{m}+\mathrm{m}}/\Delta V_{2\mathrm{m}+\mathrm{m}}$ and $\Delta V_{\mathrm{m}+\mathrm{m}+\mathrm{m}+\mathrm{m}}/\Delta V_{3\mathrm{m}+\mathrm{m}}$ are 2.5 and 6.0, respectively.

The calculated PMFs can be identified with $W(r_{12})$, $W(r_{12}, r_{13}, r_{23})$, $W(r_{12}, r_{13}, r_{23}, r_{14}, r_{24}, r_{34})$ of Eq. (4) for two, three and four solute molecules, respectively, and should, therefore, tend to zero with increasing distance (after subtracting the constant factor accounting for the hydrophobic-hydration free energy of an *isolated* solute molecule). The region 11.0–12.5 Å was used as a baseline to superimpose the PMFs of the trimer and tetramer onto that of the dimer.

Based on Eqs. (4) and (5) and the symmetry of the selected systems, we expressed the cooperative terms per pair of interactive methane molecules for systems 2m+m, m+m+m, 3m+m and m+m+m+m as follows:

$$\delta F^{(3)}_{2\mathrm{m}+\mathrm{m}}(\xi) = W^{(3)}_{2\mathrm{m}+\mathrm{m}}(\xi)/2 - W^{(2)}_{\mathrm{m}+\mathrm{m}}(\xi) \tag{18}$$

$$\delta F^{(3)}_{\mathrm{m}+\mathrm{m}+\mathrm{m}}(\xi) = W^{(3)}_{\mathrm{m}+\mathrm{m}+\mathrm{m}}(\xi)/3 - W^{(2)}_{\mathrm{m}+\mathrm{m}}(\xi) \tag{19}$$

$$\begin{aligned}\delta F^{(3,4)}_{3\mathrm{m}+\mathrm{m}}(\xi) &= \delta F^{(4)}_{3\mathrm{m}+\mathrm{m}} + 3\delta F^{(3)}_{2\mathrm{m}+\mathrm{m}} \\ &= W^{(4)}_{3\mathrm{m}+\mathrm{m}}(\xi)/3 - W^{(2)}_{\mathrm{m}+\mathrm{m}}(\xi)\end{aligned} \tag{20}$$

$$\delta F^{(4)}_{3m+m}(\xi) = W^{(4)}_{3m+m}(\xi)/3 - W^{(3)}_{2m+m}(\xi) + W^{(2)}_{m+m}(\xi) \quad (21)$$

$$\delta F^{(3,4)}_{m+m+m+m}(\xi) = \delta F^{(4)}_{m+m+m+m} + 4\delta F^{(3)}_{m+m+m} = W^{(4)}_{m+m+m+m}(\xi)/6 - W^{(2)}_{m+m}(\xi) \quad (22)$$

$$\delta F^{(4)}_{m+m+m+m}(\xi) = W^{(4)}_{m+m+m+m}(\xi)/6 - \frac{2}{3}W^{(3)}_{m+m+m}(\xi) + W^{(2)}_{m+m}(\xi) \quad (23)$$

where $\delta F^{(3,4)}$ denotes the total cooperative contribution to the PMF.

2.3. Computing molecular surface and cooperative contributions to it

The molecular surfaces of the m+m, 2m+m, m+m+m, 3m+m and m+m+m+m systems were calculated numerically using a standard triangulation method implemented in the MOLMOL program [66] with a radius $r_o = 2.09$ Å for the methane molecule and a radius 1.4 Å of the water probe.

By analogy to Eqs. (18)–(23), the cooperative contributions to the molecular surface area of systems 2m+m, m+m+m, 3m+m and m+m+m+m are defined by Eqs. (24)–(29), respectively:

$$\delta S^{(3)}_{2m+m}(\xi) = \bar{S}^{(3)}_{2m+m}(\xi)/2 - \bar{S}^{(2)}_{m+m}(\xi) \quad (24)$$

$$\delta S^{(3)}_{m+m+m}(\xi) = \bar{S}^{(3)}_{m+m+m}(\xi)/3 - \bar{S}^{(2)}_{m+m}(\xi) \quad (25)$$

$$\delta S^{(3,4)}_{3m+m}(\xi) = \delta S^{(4)}_{3m+m} + 3\delta S^{(3)}_{2m+m} = \bar{S}^{(4)}_{3m+m}(\xi)/3 - \bar{S}^{(2)}_{m+m}(\xi) \quad (26)$$

$$\delta S^{(4)}_{3m+m}(\xi) = \bar{S}^{(4)}_{3m+m}(\xi)/3 - \bar{S}^{(3)}_{2m+m}(\xi) + \bar{S}^{(2)}_{m+m}(\xi) \quad (27)$$

$$\delta S^{(3,4)}_{m+m+m+m}(\xi) = \delta S^{(4)}_{m+m+m+m} + 4\delta S^{(3)}_{m+m+m} = \bar{S}^{(4)}_{m+m+m+m}(\xi)/6 - \bar{S}^{(2)}_{m+m}(\xi) \quad (28)$$

$$\bar{S}^{(4)}_{m+m+m+m}(\xi) = \bar{S}^{(4)}_{m+m+m+m}(\xi)/6 - \frac{2}{3}\bar{S}^{(3)}_{m+m+m}(\xi) + \bar{S}^{(2)}_{m+m}(\xi) \quad (29)$$

where $\delta S^{(3,4)}$ denotes the total cooperative contribution to the molecular surface and $S^{(n)}$ denotes the normalized molecular surface of the cluster of n solute molecules.

$$\bar{S}^{(n)} = S^{(n)} - nS^{\circ} \quad (30)$$

with $S^{o} = 4\pi r_o^2$ being the molecular surface of a single solute particle.

3. Results and discussion

3.1. Two-body PMF

Although we computed and discussed the two-body PMF of the methane–methane interaction in our previous work [37], as mentioned in Section 1, in this study we extended the size of the box. Consequently, the methane–methane distance ranged up to 12.5 Å in order to address the baseline issue. The PMF is shown in Fig. 2. It can be seen that the PMF converges very well as the number of data increases.

The PMF has a characteristic shape with one deep contact minimum at 3.9 Å, a solvent-separated minimum at approximately 7 Å, corresponding to the distance at which precisely one water molecule can enter the space between the two solutes [20], and the second (very shallow) solvent-separated minimum at approximately 10 Å. The second solvent-separated minimum was out of the distance range covered in our previous study [37]. At larger distances the plot is almost flat. The baseline can thus be established by averaging the PMF at distances greater than 11 Å and its estimated error cannot exceed the depth of the second solvent-separated minimum, i.e. approximately 0.05 kcal/mol; it should be noted that this is the upper estimate of the error and the actual error is very likely to be much smaller. It should also be noted that the zero baseline estimate of our earlier work [37] corresponding to the PMF at distances close to 9 Å almost exactly matches the current zero

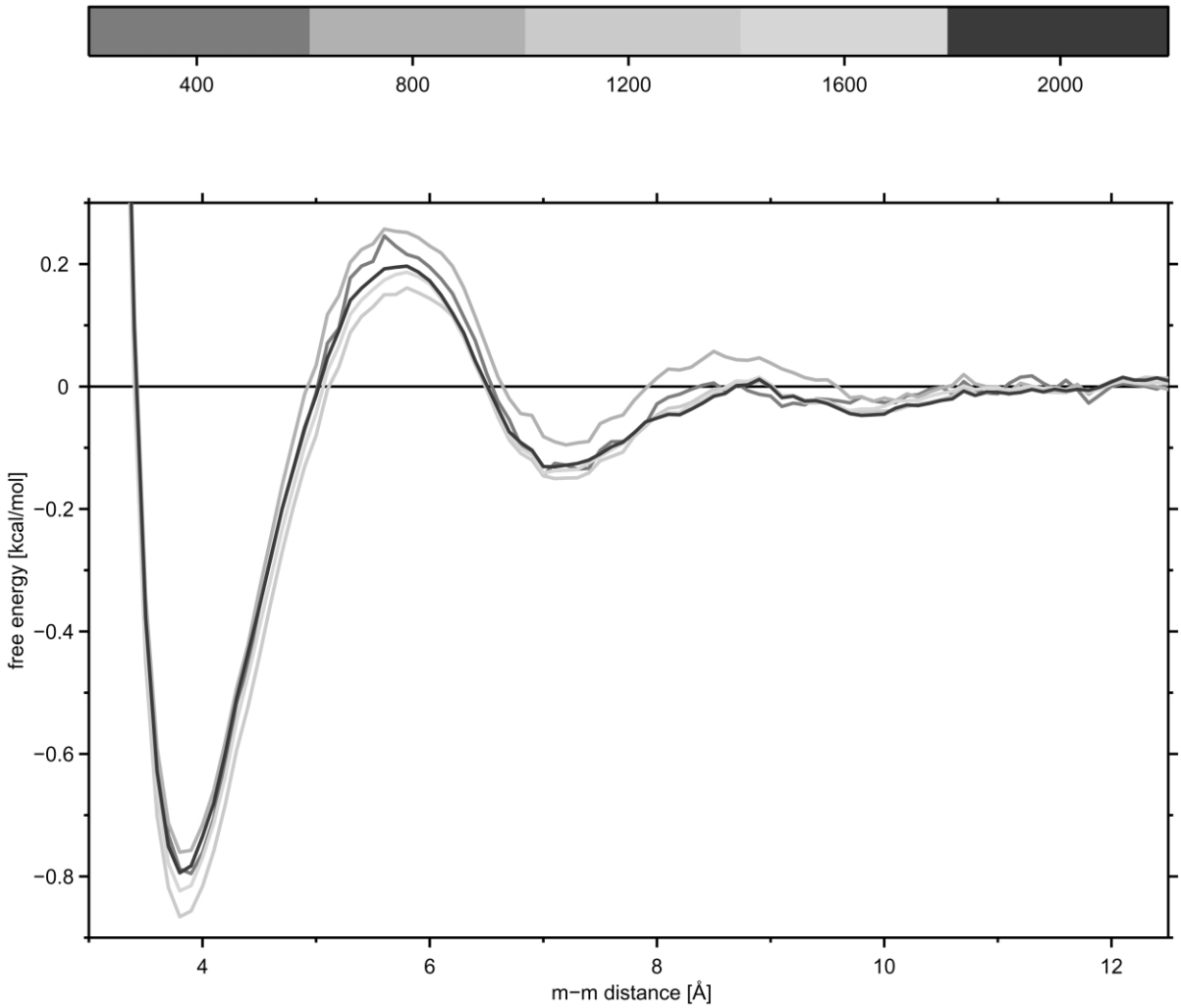

Fig. 2. PMF curves for increasing number of data for the m+m system. The colors in the upper bar denote the duration of a run (in picoseconds) in each window.

baseline obtained based on the PMF in a broader range of distances (Fig. 2). Based on the fact that the correlation functions in liquids and, consequently, the corresponding PMF's show fading and no increasing oscillations, it is very unlikely that the estimated baseline has a gross error. Thus, the criticism of our approach expressed by Shimizu and Chan [38,41] does not seem to be justified.

3.2. Three-body PMF's and cooperative terms

As in our previous work, we considered two systems: (i) a methane molecule approaching a methane dimer along the symmetry axis (2m+m; Fig. 1); and (ii) three methane molecules in an equilateral triangle configuration (m+m+m; Fig. 1). In the first case, the reaction coordinate was the distance of the third methane molecule from each of the components of the dimer, the distance between the methane molecules of the dimer being harmonically constrained at 3.9 Å, while in the second case, the reaction coordinate was the side of the triangle. The PMF curves obtained for an increasing number of data points are shown in Fig. 3a,b, respectively.

It can be seen that the convergence is reasonable, although the oscillations are larger than in the case of the two-methane PMF. This is reasonable because, although we still consider one reaction coordinate, it should be kept in mind that, in contrast to the methane–methane case, many data points do not obey the symmetry restraints. Thus, the number of data contributing to the PMF on the section of the coordinate space considered is smaller than the total number of data points. In the case of the 2m+m system, the PMF is unstable at the very end of the distance range; however, this is caused by an insufficient number of data in this region. Both the 2m+m and m+m+m PMFs exhibit three gradually shallower minima, as in the case of m+m PMF. Following the considerations of the preceding section, the upper limit of the baseline error can be estimated to be 0.05 kcal/mol.

Curves showing the converged three- and two-body PMFs as well as $\delta F^{(3)}$ are presented in Fig. 4a,b for the 2m+m and m+m+m system, respectively.

In both cases, the $\delta F^{(3)}$ curve exhibits a minimum at approximately 5 Å. The appearance of this minimum is due to the decrease in the slope of the PMF curve to the right of the contact minimum in the case of the 2m+m system, or to

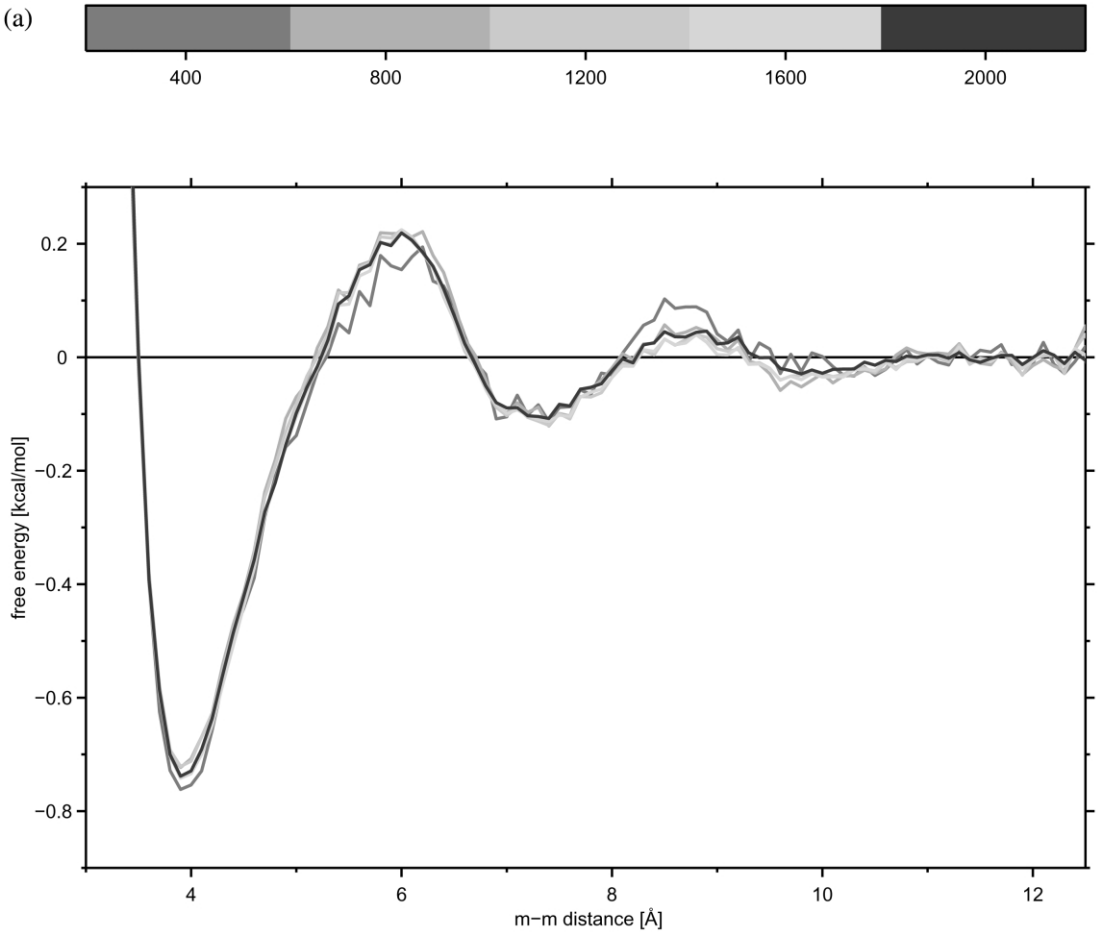

Fig. 3. The PMF curves for increasing number of data for the 2m+m (a) and m+m+m (b) system, respectively. The colors in the upper bar denote the duration of a run (in picoseconds) in each window.

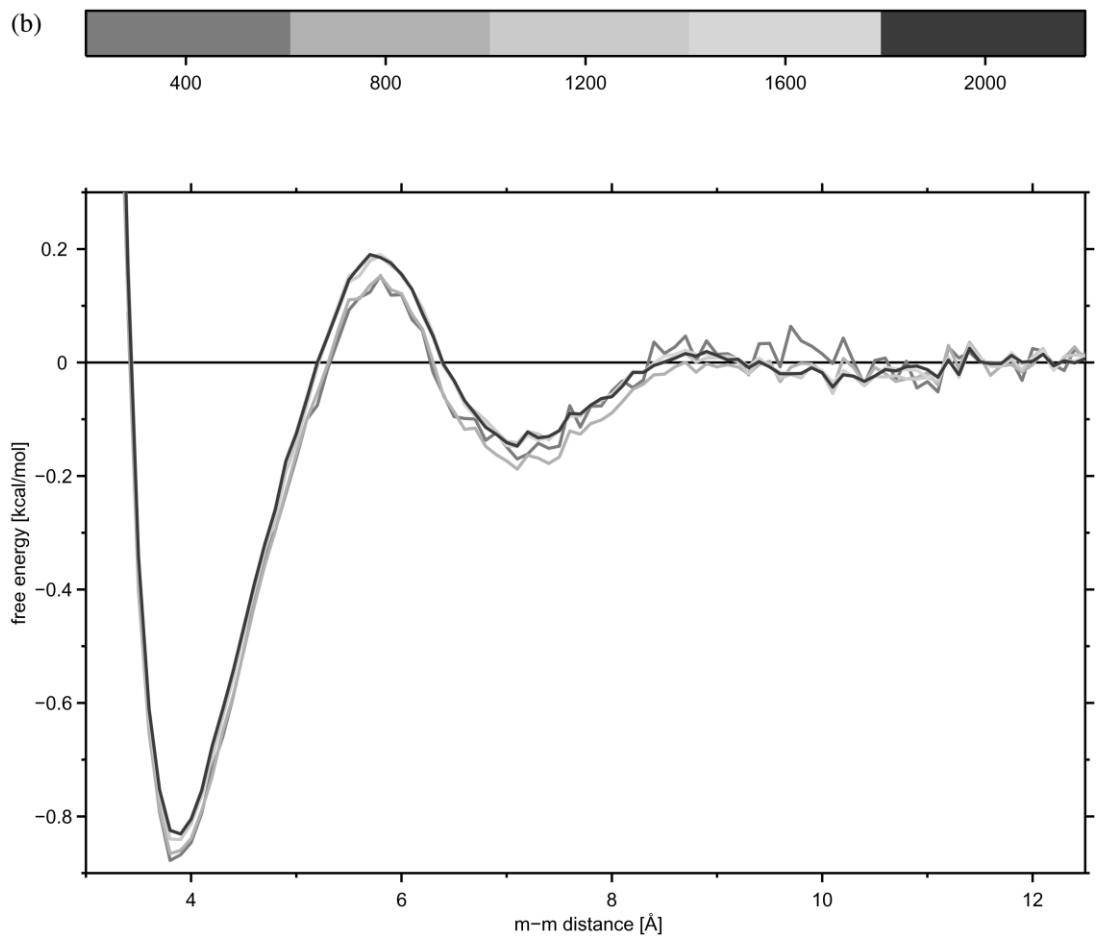

Fig. 3 (Continued).

the narrowing of the region of the maximum in the case of the m+m+m system. There is some anticooperativity near and to the left of the region of the contact minimum in the case of the 2m+m system; however, $\delta F^{(3)}$ takes on significantly positive values only at distances shorter than the contact minimum. No significant anticooperativity is observed for the m+m+m system in any distance region. For both systems, $\delta F^{(3)}$ exhibits slightly positive values past the maximum; however, these values are within the estimated baseline error and we, therefore, refrain from discussing this phenomenon in detail. The overall shape of the $\delta F^{(3)}$ curve is very similar to that of our previous work (Fig. 8 in Ref. [37]) and in the latest paper of Shimizu and Chan [42] except that their curve is shifted up by approximately 0.1 kcal/mol.

As found in our previous study [37], both for the 2m+m and the m+m+m system, the three-body contribution to the PMF is small and amounts to approximately 10% of the total PMF at the minimum. Thus, a pairwise approximation of the PMF seems to be almost sufficient in this case.

3.3. Four-body PMFs and cooperative terms

The convergence plots for the 3m+m and m+m+m+m systems are displayed in Fig. 5a,b, respectively. Due to the two-fold increase in

dimensionality of the system compared to the three-body case, we had to use a 0.2 Å bin size; otherwise the length of the simulation and the amount of data stored would have to be increased by a factor of $2^6=64$, which is unaffordable. It can be seen that the convergence is very good with little oscillation of the curves.

The four-body PMFs are plotted together with the two-body PMFs and $\delta F^{(3)}$, $\delta F^{(4)}$ and $\delta F^{(3,4)}$ (the total cooperative contribution) in Fig. 6. It can be seen that, the PMF curve of the m+m+m+m system is qualitatively similar to those of the m+m, m+m+m and 2m+m systems, with all three (contact, solvent-separated and second solvent-separated) minima present (Fig. 6b). In contrast to this, the second solvent-separated minimum of the 3m+m system (Fig. 6a) is effectively absent and the PMF is flat past the region of the first solvent-separated minimum. The first solvent-separated minimum itself is also much shallower for the 3m+m system compared to the m+m+m+m system.

Inspection of the plots in Fig. 6 reveals that, in contrast to the three-body case the cooperative effects are clearly significant. The cooperativity is manifested as substantial lowering of the first maximum and reduction of the slope in the region to the left of it. The total cooperativity curve ($\delta F^{(3,4)}$) shows a minimum of approximately 0.2 kcal/mol deep, which constitutes 25% of the depth of the contact minimum. As in the three-body case, the cooperativity is nearly zero at the contact minimum and there is anticooperativity for distances less than the contact minimum. The $\delta F^{(3,4)}$ curve of the 3m+m system takes slightly positive values in the region of the solvent-separated minimum and to the left of it and then decays smoothly to zero. There is no significant positive region past

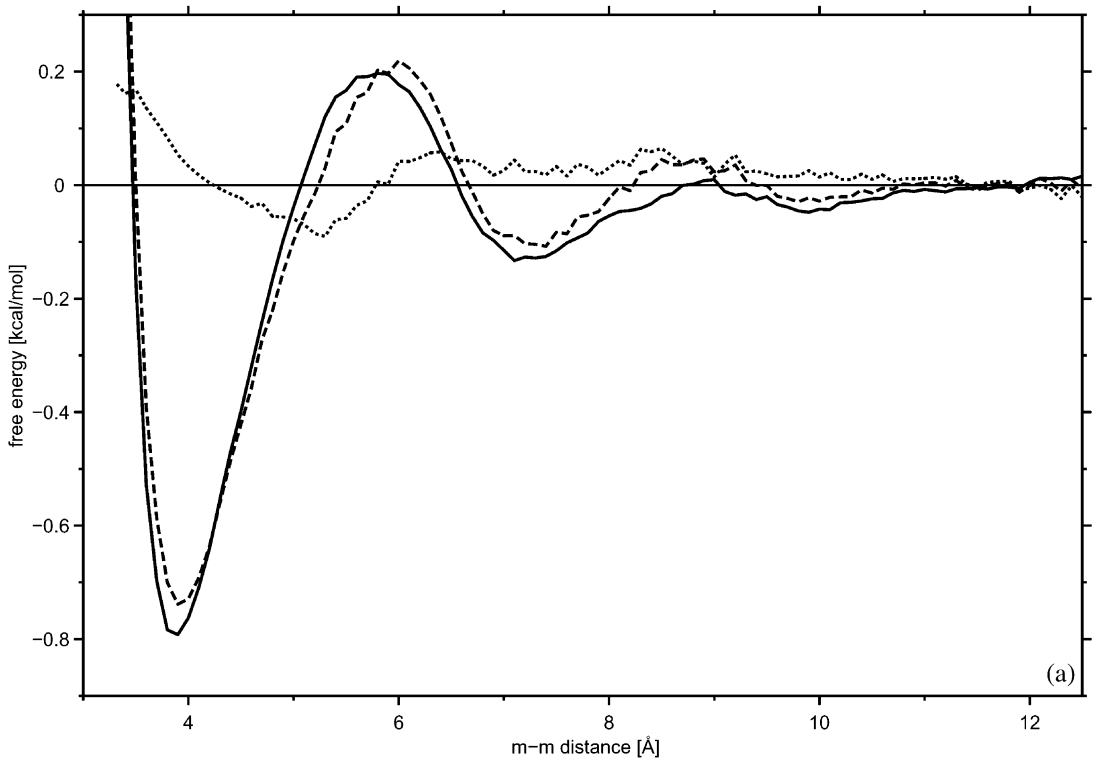

Fig. 4. Curves for the PMF and the cooperative term $\delta F^{(3)}$ for the 2m+m (a) and m+m+m (b) system, respectively. Solid lines: dimer PMF; dashed lines: trimer PMF; dotted lines: three-body contributions to the PMF.

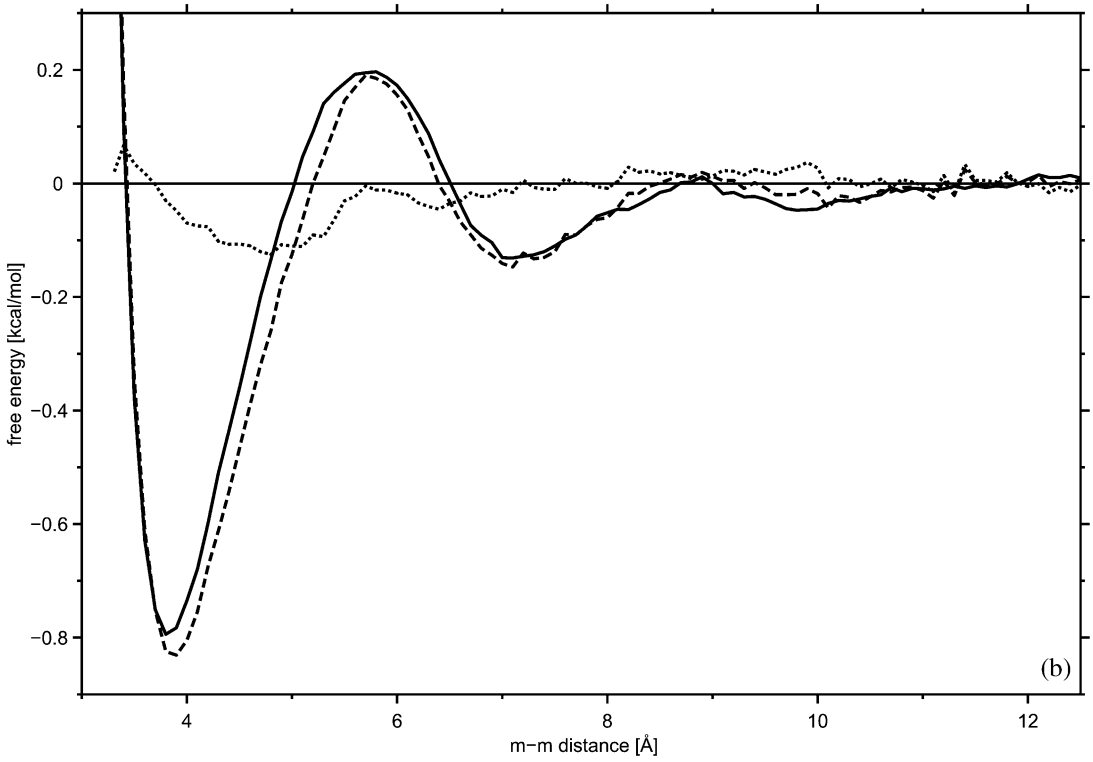

Fig. 4 (Continued).

the minimum in the $\delta F^{(3,4)}$ curve for the m+m+m+m system. The four-body cooperativity contribution, $\delta F^{(4)}$, is negative over the whole distance range. At distances farther than the solvent-separated minimum, the $\delta F^{(4)}$ curves exhibit some oscillations, which is understandable in terms of accumulation of errors (these curves are a result of a linear combination of the two-, three- and four-body PMFs).

The case of the 3m+m system is different from that of the m+m+m+m one in the region of the solvent-separated minimum, which is shallower for the 3m+m system than that of the m+m system (Fig. 6a). This results in a maximum of $\delta F^{(3,4)}$ and, consequently, anticooperativity in the region of the solvent-separated minimum. Thus, the multibody contributions act to flatten the structure of the PMF beyond the region of the contact minimum. This facilitates the approach of a hydrophobic particle to the trimer: it will have less chance to be trapped in the solvent-separated minimum and will encounter a lower barrier on approach to the contact minimum. A similar difference can be observed between the PMFs of the 2m+m and m+m+m systems; however, the flattening of the solvent-separated minimum is small and is contained within the estimated error of the simulations (Fig. 4).

It should be noted that, in the case of the four-methane systems, the existence of the cooperativity in hydrophobic association can be assessed independent of the baseline. The difference between the contact minimum and the maximum is 0.99 kcal/mol for the m+m system and decreased to 0.79 kcal/mol for the 3m+m and 0.86 kcal/mol for the m+m+m+m system, respectively. Thus, a significant decrease of the barrier between the contact- and solvent-separated minimum due to multibody interaction is apparent, which in turn means that there is cooperativity in the region of

this barrier. Inspection of Fig. 6 shows that lowering of the barrier is due to the four-body contributions.

3.4. Comparison of the cooperative terms in the PMFs with molecular surface area

Rank and Baker [36] observed that the solvent contribution to the PMF of association of two hydrophobic solutes has a qualitatively similar distance dependence as the molecular surface area of the associating particles. In our previous work [37,39], we extended this observation to the three-body cooperative contribution to the PMF. We, therefore, thought it worthwhile to compare the distance dependence of the cooperative contributions to the PMFs of the 3m+m and m+m+m+m systems with those of the molecular surface area of these two systems. The respective plots are presented in Fig. 7a,b. It can be seen that, in the case of the m+m+m+m system, both the total multibody contribution to the surface area, $\delta S^{(3,4)}$, and its components, $\delta S^{(3)}$ and $\delta S^{(4)}$ agree very well with $\delta F^{(3,4)}$, $\delta F^{(3)}$ and $\delta F^{(4)}$, respectively. In both cases, the curve expressing the total multibody effect has a broad minimum approximately 5 Å, the curve corresponding to three-body contribution is shifted to the left, while the four-body contribution has a sharper minimum at approximately 5.5 Å. The curves of δS for the 3m+m system also agree with the corresponding curves for δF; however, the agreement between the relations of the depths of the minima is not as good as in the case of the m+m+m+m system. This might be due to the fact that the errors are more significant in the case of the 3m+m system, compared to those for the m+m+m+m system Eqs. (16) and (17).

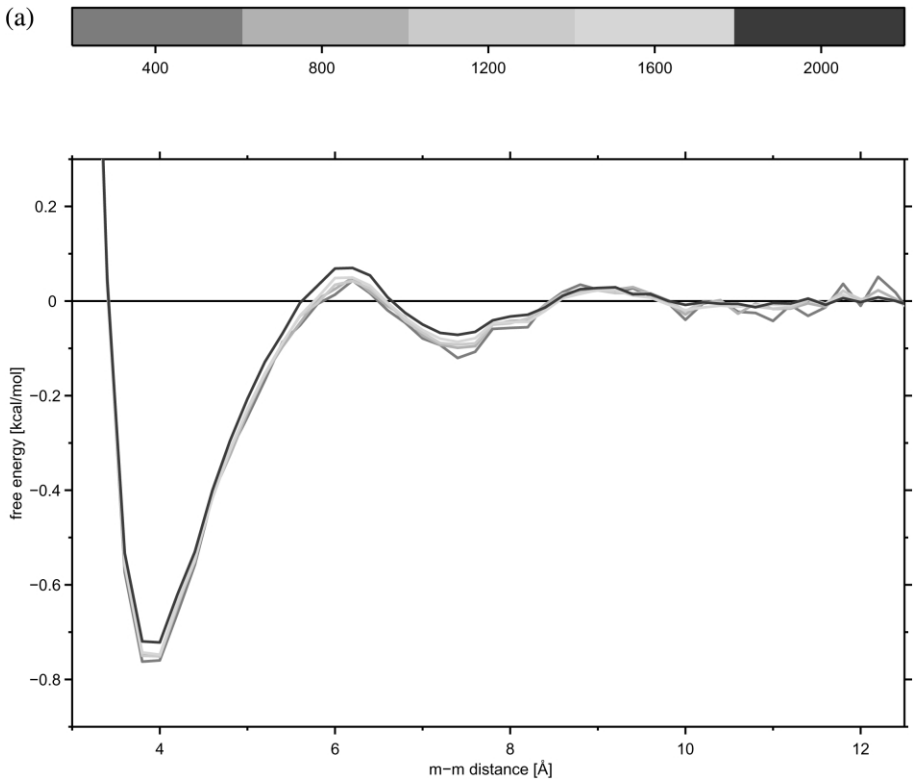

Fig. 5. The PMF curves for increasing number of data for the 3m+m (a) and m+m+m+m (b) system, respectively. The colors in the upper bar denote the duration of a run (in picoseconds) in each window.

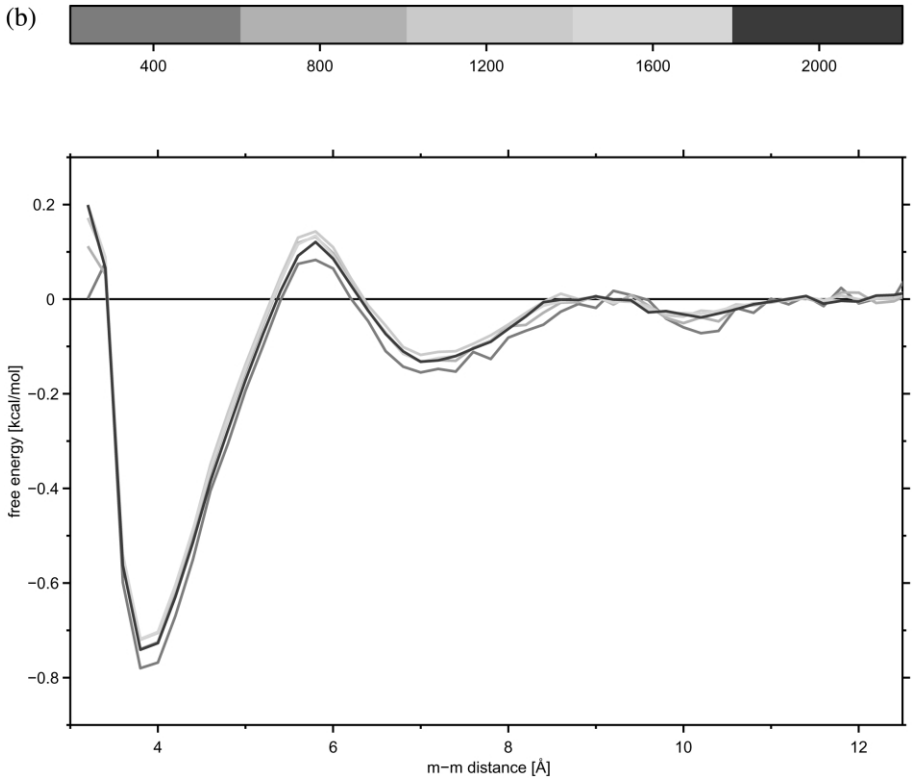

Fig. 5 (Continued).

4. Conclusions

The results reported in this paper show that, in the case of the four-methane clusters, the multibody contribution to hydrophobic association is significantly greater compared to the case of three-methane clusters studied in our earlier work [37,40] and by other authors [36,38,42]. The cooperativity is manifested as a lowering of the desolvation barrier by 0.07 kcal/mol (for the 3m+m system) and 0.11 kcal (for the m+m+m+m system), respectively; this lowering is due to the four-body contributions. The distance dependence of the multibody contributions to the PMF is in excellent agreement with that of the molecular surface area, which confirms the observation of Rank and Baker [36] that molecular surface area provides a good description of hydrophobic solvation.

Our results provide the answer to the criticism of Shimizu and Chan [38] regarding the methods used by us to study the hydrophobic effect. While we can determine only the relative values of the free energy by using umbrella sampling with WHAM, extension of the distance range in this study showed that the baseline of the PMF is well established, and the sign of the cooperative effect can be judged unambiguously. Any long-range effects postulated by Shimizu and Chan seem to be covered within the random error inherent in the simulations, whose upper bound is estimated to be 0.05 kcal/mol. Moreover, the sign of the multibody contribution to the PMF of hydrophobic association of both four-methane clusters studied, calculated as the difference between the height of the maximum and the depth of the contact minimum is independent of the choice of the baseline. Our results show that this difference decreases by

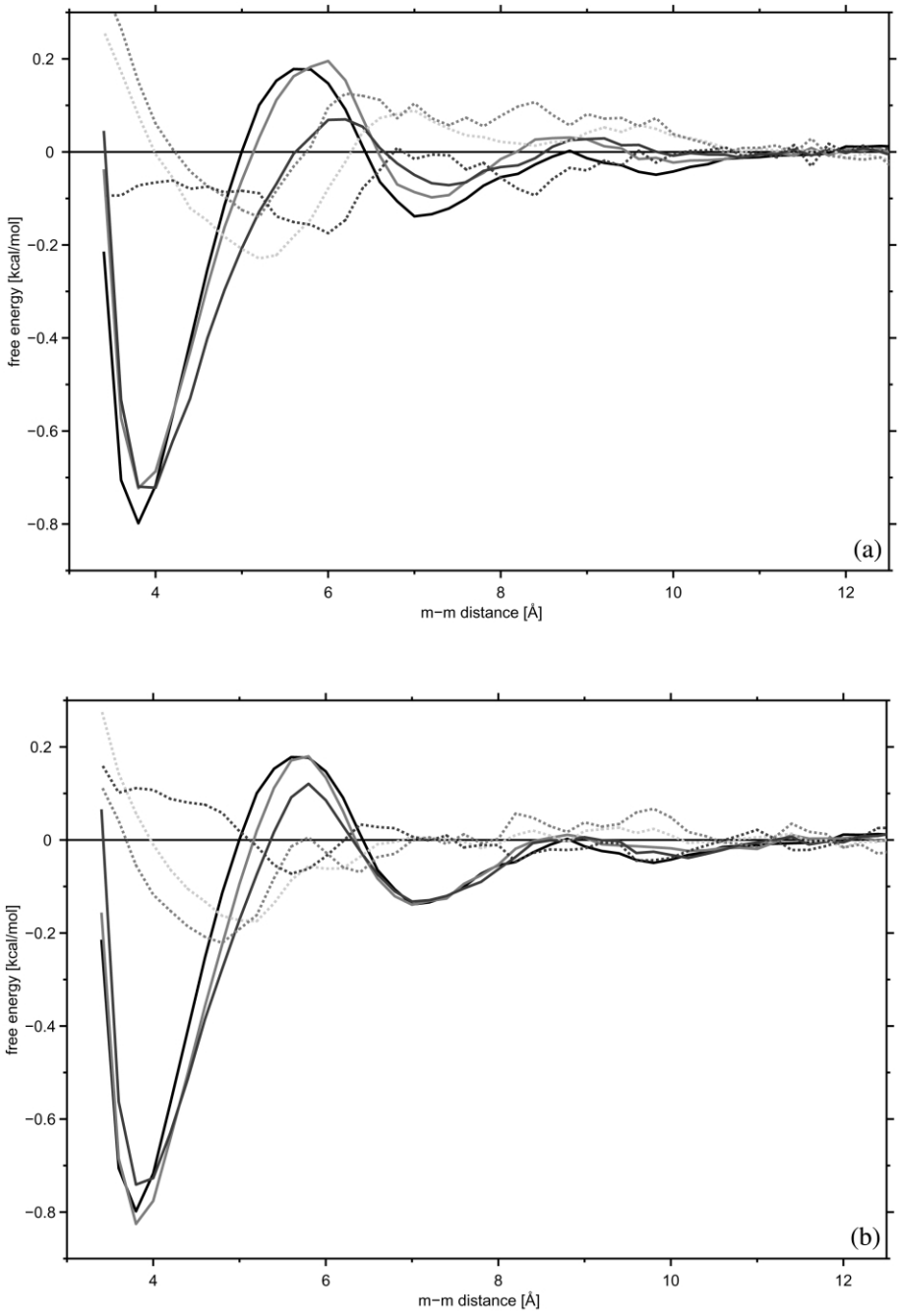

Fig. 6. Curves for the PMF and the cooperative terms $\delta F^{(3,4)}$, $\delta F^{(3)}$ and $\delta F^{(4)}$ for the 3m+m (a) and m+m+m+m (b) system, respectively. Black: dimer PMF; red: trimer PMF; blue: tetramer PMF; dotted green line: total cooperative contribution [$\delta F^{(3,4)}$] to the tetramer PMF; dotted red line: three-body contribution [$\delta F^{(3)}$] to the tetramer PMF; dotted blue line: four-body contribution ($\delta F^{(4)}$) to the tetramer PMF.

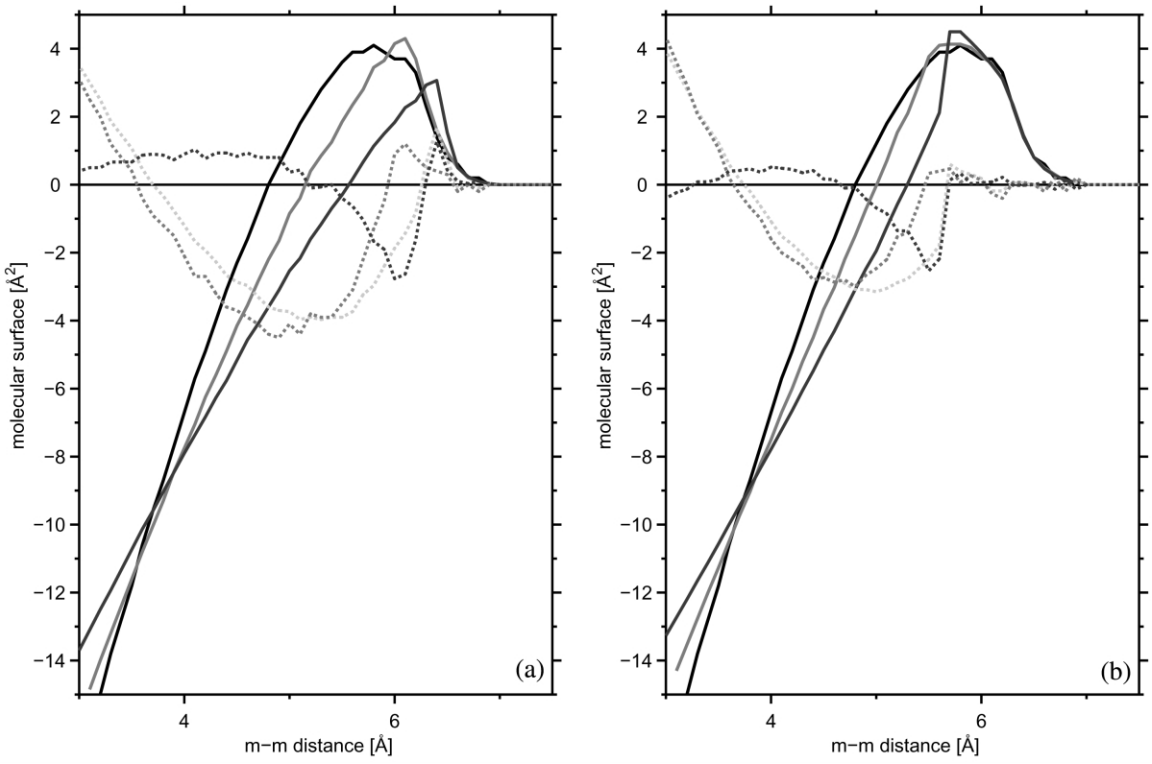

Fig. 7. Distance dependence of the molecular surface area and its decomposition into multibody terms for the 3m+m (a) and m+m+m+m (b) system, respectively. The color scheme is the same as for Fig. 6.

approximately 0.2 kcal/mol for four-methane compared to two-methane systems, which clearly indicates cooperativity in hydrophobic interaction. Furthermore, Shimizu and Chan mainly address the value of the multibody contribution to the PMF at the contact minimum. It should be noted that our results show that the contribution to the PMF at the contact minimum (3.9 Å) can be slightly positive, although it is most likely to be nearly zero given the error estimate, but is negative at distances of approximately 5 Å.

Finally, it should be noted that four-methane clusters provide a much better test case than methane trimers. In our earlier work [40], we also demonstrated that trimers of larger solutes exhibit greater cooperativity than methane trimers. It is likely that yet more pronounced cooperative contributions to the PMF can be captured in tetramers of larger solutes or higher associates of methane molecules. Also, a determination of the PMF's of hydrocarbons, which are parts of amino-acid side chains, will find more application in theoretical studies of protein folding. This is currently under investigation in our laboratory.

Acknowledgments

This work was supported by grants from the National Institutes of Health (GM-14312), the National Science Foundation (MCB00-03722), the Fogarty Foundation (TW1064) and grant BW/8000-5-0170-1 from the Polish State Committee for Scientific Research (KBN). Support was also received from the National Foundation for Cancer Research. Sylwia Rodziewicz-Motowidło is a recipient of a fellowship from The Foundation for Polish Science. This research was conducted using the resources of (a) the National Science Founda-

tion Terascale Computing System at the Pittsburgh Supercomputer Center, (b) the Informatics Center of the Metropolitan Academic Network (IC MAN) in Gdańsk and (c) our own 40-processor Linux cluster at the Faculty of Chemistry, University of Gdańsk.

References

[1] W. Kauzmann, Some factors in the interpretation of protein denaturation, Adv. Protein Chem. 14 (1959) 1–63.
[2] W. Kauzmann, Denaturation of proteins and enzymes, in: W. McElroy, B. Glass (Eds.), The Mechanism of Enzyme Action, The Johns Hopkins Press, Baltimore, 1954, p. 70.
[3] G. Némethy, H.A. Scheraga, Structure of water and hydrophobic bonding in proteins. I. A model for the thermodynamic properties of liquid water, J. Chem. Phys. 36 (1962) 3382–3400.
[4] J.C. Owicki, H.A. Scheraga, Monte Carlo calculations in the isothermal-isobaric ensemble. 2. Dilute aqueous solution of methane, J. Am. Chem. Soc. 99 (1977) 7413–7418.
[5] R.H. Kincaid, H.A. Scheraga, Acceleration of convergence in Monte Carlo simulations of aqueous solutions using the Metropolis algorithm. Hydrophobic hydration of methane, J. Comput. Chem. 3 (1982) 525–547.
[6] W. Blokziji, J.B.F.N. Engberts, Hydrophobic effects: opinions and facts, Angew. Chem. Int. Ed. Engl. 32 (1993) 1545–1579.
[7] H.A. Scheraga, G. Némethy, I.Z. Steinberg, The contribution of hydrophobic bonds to the thermal stability of protein conformations, J. Biol. Chem. 237 (1962) 2506–2508.
[8] D.C. Poland, H.A. Scheraga, Hydrophobic bonding and micelle stability, J. Phys. Chem. 69 (1965) 2431–2442.
[9] A. Ben-Naim, Hydrophobic Interactions, Plenum Press, New York, 1980.
[10] G. Ravishanker, D.L. Beveridge, Theoretical studies of the hydrophobic effect, in: G. Náray-Szabó (Ed.), Theoretical Chemistry of Biological Systems, Chapter 7, Elsevier, Amsterdam, 1986, pp. 423–494.
[11] H.A. Scheraga, Theory of hydrophobic interactions, J. Biomol. Struct. Dyn. 16 (1998) 447–460.
[12] A. Ben-Naim, Solvent-induced interactions: hydrophobic and hydrophilic phenomena, J. Chem. Phys. 90 (1989) 7412–7425.
[13] A. Ben-Naim, R. Mazo, Size dependence of solvation Gibbs energies: A critique and a rebuttal of some recent publications, J. Phys. Chem. B 101 (1997) 11221–11225.
[14] Y. Sun, P. Kollman, Are there water-bridge-induced hydrophilic interactions, J. Phys. Chem. 100 (1996) 6760–6763.
[15] H.S. Frank, M.W. Evans, Free volume and entropy in condensed systems. III. Entropy in binary liquid mixtures; partial molal entropy in dilute solutions; structure and thermodynamics in aqueous electrolytes, J. Chem. Phys. 13 (1945) 507–532.
[16] H.S. Frank, W.Y. Wen, Structural aspects of ion-solvent interaction in aqueous solutions—a suggested picture of water structure, Disc. Faraday Soc. 24 (1957) 133–140.
[17] G. Némethy, H.A. Scheraga, Structure of water and hydrophobic bonding in proteins. IV. The thermodynamic properties of liquid deuterium oxide, J. Chem. Phys. 41 (1964) 680–689.
[18] G. Némethy, H.A. Scheraga, Structure of water and hydrophobic bonding in proteins. II. A model for the thermodynamic properties of aqueous solutions of hydrocarbons, J. Chem. Phys. 36 (1962) 3401–3417.
[19] G. Némethy, H.A. Scheraga, The structure of water and hydrophobic bonding in proteins. III. The thermodynamic properties of hydrophobic bonds in proteins. J. Phys. Chem. 66 (1962) 1773–1789. Erratum: J. Phys. Chem. 67 (1963) 2888.
[20] A. Geiger, A. Rahman, F.H. Stillinger, Molecular dynamics study of the hydration of Lennard–Jones solutes, J. Chem. Phys. 70 (1979) 263–276.
[21] D.C. Rapaport, H.A. Scheraga, Hydration of inert solutes. A molecular dynamics study, J. Phys. Chem. 86 (1982) 873–880.
[22] F.H. Stillinger, Structure in aqueous solutions of nonpolar solutes from the standpoint of scaled-particle theory, J. Solut. Chem. 2 (1973) 141–158.
[23] N.T. Southall, K.A. Dill, The mechanism of hydrophobic solvation depends on solute radius, J. Phys. Chem. B 104 (2000) 1326–1331.
[24] N.T. Southall, K.A. Dill, A.D.J. Haymet, A view of the hydrophobic effect, J. Phys. Chem. B 106 (2002) 521–533.
[25] K. Lum, D. Chandler, J.D. Weeks, Hydrophobicity at small and large length scales, J. Phys. Chem. B 103 (1999) 4570–4577.
[26] R.H. Wood, P.T. Thompson, Differences between pair and bulk hydrophobic interactions, Proc. Natl. Acad. Sci. 87 (1990) 946–949.
[27] S. Lüdemann, R. Abseher, H. Schreiber, O. Steinhauser, The temperature-dependence of hydrophobic association in water. Pair versus bulk hydrophobic interactions, J. Am. Chem. Soc. 119 (1997) 4206–4213.
[28] D.E. Smith, A.D.J. Haymet, Free energy, entropy, and internal energy of hydrophobic interactions: computer simulations, J. Chem. Phys. 98 (1993) 6445–6454.
[29] D. van Belle, S.J. Wodak, Molecular dynamics study of methane hydration and methane association in a polarizable water phase, J. Am. Chem. Soc. 115 (1993) 647–652.
[30] W.S. Young, C.L. Brooks III, A reexamination of the hydrophobic effect: exploring the role of the solvent model in computing the methane–methane potential of mean force, J. Chem. Phys. 106 (1997) 9265–9269.

[31] S. Lüdemann, H. Schreiber, R. Abseher, O. Steinhauser, The influence of temperature on pairwise hydrophobic interactions of methane-like particles: a molecular dynamics study of free energy, J. Chem. Phys. 104 (1996) 286–295.

[32] S. Shimizu, H.S. Chan, Temperature dependence of hydrophobic interactions: a mean force perspective, effects of water density, and non-additivity of thermodynamic signatures, J. Chem. Phys. 113 (2000) 4683–4700.

[33] P.-L. Chau, R.L. Mancera, Computer simulation of the structural effect of pressure on the hydrophobic hydration of methane, Mol. Phys. 96 (1999) 109–122.

[34] T. Ghosh, A.E. Garcia, S. Garde, Enthalpy and entropy contributions to the pressure dependence of hydrophobic interactions, J. Chem. Phys. 116 (2002) 2480–2486.

[35] R.L. Mancera, Does salt increase the magnitude of the hydrophobic effect? A computer simulation study, Chem. Phys. Lett. 296 (1998) 459–465.

[36] J.A. Rank, D. Baker, A desolvation barrier to hydrophobic cluster formation may contribute to the rate-limiting step in protein folding, Protein Sci. 6 (1997) 347—354.

[37] C. Czaplewski, S. Rodziewicz-Motowidło, A. Liwo, D.R. Ripoll, R.J. Wawak, H.A. Scheraga, Molecular simulation study of cooperativity in hydrophobic association, Protein Sci. 9 (2000) 1235–1245.

[38] S. Shimizu, H.S. Chan, Anti-cooperativity in hydrophobic interactions: a simulations study of spatial dependence of three body effects and beyond, J. Chem. Phys. 115 (2001) 1414–1421.

[39] C. Czaplewski, S. Rodziewicz-Motowidło, A. Liwo, D.R. Ripoll, R.J. Wawak, H.A. Scheraga, Comment on 'Anti-cooperativity in hydrophobic interactions: a simulation study of spatial dependence of three-body effects and beyond', J. Chem. Phys. 115 (2001) 1414, 115 (2001) 1414, J. Chem. Phys. 116 (2002) 2665–2667.

[40] C. Czaplewski, D.R. Ripoll, A. Liwo, S. Rodziewicz-Motowidło, R.J. Wawak, H.A. Scheraga, Can cooperativity of hydrophobic association be reproduced correctly by implicit solvation models?, Int. J. Quant. Chem. 88 (2002) 41–55.

[41] S. Shimizu, H.S. Chan, Reply to ''Comment on 'Anti-cooperativity in hydrophobic interactions: a simulation study of spatial dependence of three-body effects and beyond' '', J. Chem. Phys. 116 (2002) 2665, 116 (2002) 2665, J. Chem. Phys. 116 (2002) 2668–2669.

[42] S. Shimizu, H.S. Chan, Anti-cooperativity and cooperativity in hydrophobic interactions: three-body free energy landscape and comparison with implicit-solvent potential functions for proteins, Proteins Struct. Funct. Genet. 48 (2002) 15–30.

[43] F. Bruge, S.L. Fornili, G.G. Malenkov, M.B. Palma-Vittorelli, M.U. Palma, Solvent-induced forces on molecular scale: non-additivity, modulation and causal relation to hydration, Chem. Phys. Lett. 254 (1996) 283–291.

[44] P.L. San Biagio, D. Bulone, V. Martorana, M.B. Palma-Vittorelli, M.U. Palma, Physics and biophysics of solvent induced forces: hydrophobic interactions and context-dependent hydration, Eur. Biophys. J. 27 (1998) 183–196.

[45] J. Tsai, M. Gerstein, M. Levitt, Simulating the minimum core for hydrophobic collapse in globular proteins, Protein Sci. 6 (1997) 2606–2616.

[46] T.M. Raschke, J. Tsai, M. Levitt, Quantification of the hydrophobic interactions by simulations of the aggregation of small hydrophobic solutes in water, Proc. Natl. Acad. Sci. USA 98 (2001) 5965–5969.

[47] M.R. Betancourt, D. Thirumalai, Pair potentials for protein folding: choice of reference states and sensitivity of predicted native states to variations in the interactions schemes, Protein Sci. 8 (1999) 361–369.

[48] M. Vendruscolo, R. Najmanovich, E. Domany, Can a pairwise contact potential stabilize native protein folds against decoys obtained by threading?, Proteins Struct. Funct. Genet. 38 (2000) 134–148.

[49] D. Tobi, R. Elber, Distance-dependent, pair potential for protein folding: results from linear optimization, Proteins Struct. Funct. Genet. 41 (2000) 40–46.

[50] A. Koliński, A. Godzik, J. Skolnick, A general method for the prediction of the three-dimensional structure and folding pathway of globular proteins: application to designed helical proteins, J. Chem. Phys. 98 (1993) 7420–7433.

[51] A. Godzik, A. Koliński, J. Skolnick, De novo and inverse folding predictions of protein structure and dynamics, J. Comput. Aid. Mol. Des. 7 (1993) 397–438.

[52] A. Koliński, W. Galazka, J. Skolnick, On the origin of the cooperativity of protein folding: implications from model simulations, Proteins Struct. Funct. Genet. 26 (1996) 271–287.

[53] A. Liwo, C. Czaplewski, J. Pillardy, H.A. Scheraga, Cumulant-based expressions for the multibody terms for the correlation between local and electrostatic interactions in the united-residue (UNRES) force field, J. Chem. Phys. 115 (2001) 2323–2347.

[54] A. Liwo, R. Kaźmierkiewicz, C. Czaplewski, M. Groth, S. Ołdziej, R.J. Wawak, et al., United-residue force field for off-lattice protein-structure simulations; III. Origin of backbone hydrogen-bonding cooperativity in united-residue potentials, J. Comput. Chem. 19 (1998) 259–276.

[55] J. Pillardy, C. Czaplewski, A. Liwo, J. Lee, D.R. Ripoll, R. Kaźmierkiewicz, et al., Recent improvements in prediction of protein structure by global optimization of a potential energy function, Proc. Nat. Acad. Sci. 98 (2001) 2329–2333.

[56] A. Liwo, J. Pillardy, R. Kaźmierkiewicz, R.J. Wawak, M. Groth, C. Czaplewski, et al., Prediction of protein structure using a knowledge-based off-lattice united-residue force field and global optimization methods, Theoret. Chem. Acc. 101 (1999) 16–20.

[57] G.M. Torrie, J.P. Valleau, Non-physical sampling distributions in Monte Carlo free-energy estimation: umbrella sampling, J. Comp. Phys. 23 (1977) 187–199.
[58] D. Frenkel, B. Smit, Understanding Molecular Simulation–From Algorithms to Applications, Chapter 7, Academic Press, San Diego, 1996, pp. 176–181.
[59] S. Kumar, D. Bouzida, R.H. Swendsen, P.A. Kollman, J.M. Rosenberg, The weighted histogram analysis method for free-energy calculations on biomolecules. I. The method, J. Comput. Chem. 13 (1992) 1011–1021.
[60] S. Kumar, J.M. Rosenberg, D. Bouzida, R.H. Swendsen, P.A. Kollman, Multidimensional free-energy calculations using the weighted histogram analysis method, J. Comput. Chem. 16 (1995) 1339–1350.
[61] W.L. Jorgensen, J. Chandrasekhar, J.D. Madura, R.W. Impey, M.L. Klein, Comparison of simple potential functions for simulating liquid water, J. Chem. Phys. 79 (1983) 926–935.
[62] W.L. Jorgensen, J.D. madura, C.J. Swenson, Optimized intermolecular potential functions for liquid hydrocarbons, J. Am. Chem. Soc. 106 (1984) 6638–6646.
[63] M.P. Alien, D.J. Tildesley, Computer Simulation of Liquids, Chapter 1.4.2, Oxford University Press, New York, 1987, p. 21.
[64] W.F. van Gunsteren, H.J.C. Berendsen, Algorithms for macromolecular dynamics and constraint dynamics, Mol. Phys. 34 (1977) 1311–1327.
[65] D.A. Pearlman, D.A. Case, J.W. Caldwell, W.S. Ross, T.E. Cheatham III, S. DeBolt, et al., Amber, a package of computer programs for applying molecular mechanics, normal mode analysis, molecular dynamics and free energy calculations to simulate the structural and energetic properties of molecules, Comp. Phys. Commun. 91 (1995) 1–41.
[66] R. Koradi, M. Billeter, K. Wüthrich, Molmol: a program for display and analysis of macromolecular structures, J. Mol. Graphics 14 (1996) 51–55.